

Factors influencing the rearrangement of *bis*-allylic hydroperoxides by manganese lipoxygenase

Ernst H. Oliw¹

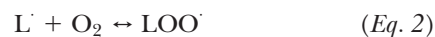
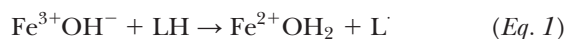
Division of Biochemical Pharmacology, Department of Pharmaceutical Biosciences, Uppsala University, Biomedical Center, SE-751 24 Uppsala, Sweden

Abstract Manganese lipoxygenase (Mn-LOX) catalyzes the rearrangement of *bis*-allylic *S*-hydroperoxides to allylic *R*-hydroperoxides, but little is known about the reaction mechanism. 1-Linoleoyl-lysoglycerophosphatidylcholine was oxidized in analogy with 18:2n-6 at the *bis*-allylic carbon with rearrangement to C-13 at the end of lipoxygenation, suggesting a “tail-first” model. The rearrangement of *bis*-allylic hydroperoxides was influenced by double bond configuration and the chain length of fatty acids. The Gly316Ala mutant changed the position of lipoxygenation toward the carboxyl group of 20:2n-6 and 20:3n-3 and prevented the *bis*-allylic hydroperoxide of 20:3n-3 but not 20:2n-6 to interact with the catalytic metal. The oxidized form, Mn^{III}-LOX, likely accepts an electron from the *bis*-allylic hydroperoxide anion with the formation of the peroxy radical, but rearrangement of 11-hydroperoxyoctadecatrienoic acid by Mn-LOX was not reduced in D₂O (pD 7.5), and aqueous Fe³⁺ did not transfer 11*S*-hydroperoxy-9*Z*,12*Z*,15*Z*-octadecatrienoic acid to allylic hydroperoxides. Mutants in the vicinity of the catalytic metal, Asn466Leu and Ser469Ala, had little influence on *bis*-allylic hydroperoxide rearrangement. **■** In conclusion, Mn-LOX transforms *bis*-allylic hydroperoxides to allylic by a reaction likely based on the positioning of the hydroperoxide close to Mn³⁺ and electron transfer to the metal, with the formation of a *bis*-allylic peroxy radical, β -fragmentation, and oxygenation under steric control by the protein.—Oliw, E. H. Factors influencing the rearrangement of *bis*-allylic hydroperoxides by manganese lipoxygenase. *J. Lipid Res.* 2008. 49: 420–428.

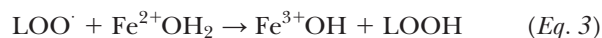
Supplementary key words electron transfer • 1-linoleoyl-lysoglycerophosphatidylcholine • mass spectrometry • metalloenzymes • peroxy radicals • *R*-lipoxygenase • solvent deuterium isotope effect • site-directed mutagenesis

Lipoxygenases constitute a gene family of nonheme metalloenzymes with conserved metal ligands, which oxygenate polyunsaturated fatty acids to hydroperoxides and related compounds (1). Lipoxygenases occur in plants and mammals and are of considerable medical and biological interest (2, 3). Lipoxygenation occurs by

hydrogen atom abstraction at the *bis*-allylic carbon of 1*Z*,4*Z*-pentadienes of fatty acids followed by O₂ insertion, with the formation of *cis-trans* conjugated (allylic) hydroperoxy fatty acids. Lipoxygenases occur in resting (reduced; Fe²⁺) and active (oxidized; Fe³⁺) forms. The active form of lipoxygenases contains the catalytic base, Fe³⁺OH⁻ (4), which forms a carbon-centered radical (L). The latter reacts with molecular oxygen and forms a peroxy radical:



In the next step, the catalytic base is regenerated, with the formation of the hydroperoxide:



Experimental and density functional studies of H atom abstraction by soybean lipoxygenase (sLO-1) suggest a proton-coupled electron transfer mechanism by which the electron and the proton are transferred separately (5–7).

Autoxidation of polyunsaturated fatty acids also occurs by the abstraction of hydrogen at *bis*-allylic carbons, with the formation of peroxy radicals, yet lipoxygenation and autoxidation differ in other respects. Lipoxygenases form *cis-trans* conjugated hydroperoxides with stereo and position selectivity, and the initial hydrogen abstraction is associated with a large kinetic isotope effect ($k_{\text{H}}/k_{\text{D}} \sim 40$) that is attributable to tunneling of the deuterium atom (8). The corresponding kinetic isotope effect during autoxidation is in agreement with classical theory ($k_{\text{H}}/k_{\text{D}} 5\text{--}6$) (9). Autoxidation of polyunsaturated fatty acids generates both unconjugated and *cis-trans* and *trans-trans* con-

Abbreviations: CP, chiral phase; DiHETrE, dihydroxyeicosatrienoic acid; GPC, glycerophosphatidylcholine; HEDE, hydroxyeicosadienoic acid; HODE, hydroxyoctadecadienoic acid; HPETE, hydroperoxyeicosatetraenoic acid; HPETrE, hydroperoxyeicosatrienoic acid; HPODE, hydroperoxyoctadecadienoic acid; HPOTrE, hydroperoxyoctadecatrienoic acid; Mn-LOX, manganese lipoxygenase; NP, normal phase; RP, reverse phase; sLO-1, soybean lipoxygenase; UV, ultraviolet.

¹ To whom correspondence should be addressed.

e-mail: ernst.oliw@farmbio.uu.se

Manuscript received 8 November 2007 and in revised form 14 November 2007.

Published, JLR Papers in Press, November 17, 2007.

DOI 10.1194/jlr.M700514-JLR200

jugated hydroperoxides (1011–12). The spin density of the carbon-centered radical is highest at the *bis*-allylic carbons (13) and the major products are formed by oxygenation at these positions. Rearrangement of these *bis*-allylic peroxy radicals to allylic radicals occurs rapidly, with a rate constant of $\sim 2 \times 10^6$, $\sim 10^5$ times faster than the rearrangement of alkyl radicals. Consequently, *bis*-allylic hydroperoxides accumulate only during autoxidation in the presence of high concentrations of hydrogen donors (e.g., α -tocopherol), which convert the *bis*-allylic peroxy radicals to the relatively stable *bis*-allylic hydroperoxides (11).

Manganese lipoxygenase (Mn-LOX) is secreted by the take-all fungus and contains Mn as the catalytic metal (14). It is the only known naturally occurring lipoxygenase that forms significant amounts (>0.5%) of *bis*-allylic hydroperoxides (15). Mn-LOX catalyzes the oxygenation of 18:2n-6 by suprafacial hydrogen abstraction at C-11 and O₂ insertion at the *bis*-allylic position C-11 and, with double bond migration, at the allylic position C-13. The enzyme produces 11*S*-hydroperoxy-9*Z*,12*Z*-octadecadienoic acid (11-HPODE) and 13*R*-hydroperoxy-9*Z*,11*E*-octadecadienoic acid (13-HPODE) at an $\sim 1:4$ ratio (15). At the end of lipoxygenation, 11-HPODE is transformed to 13-HPODE by Mn-LOX (15). Electron paramagnetic resonance analysis suggests that the catalytic metal redox cycles ($\text{Mn}^{2+}/\text{Mn}^{3+}$) between the resting and active forms of the enzyme, in analogy with Fe-lipoxygenases, and that the metal coordinating residues are virtually identical (16–19). To date, the oxygenation of *bis*-allylic carbons by Fe-lipoxygenases has only been reported for the recombinant lipoxygenase domain of allene oxide synthase of *Plexaura homomalla*, which transforms 20:3n-6 to the *bis*-allylic hydroperoxide at C-10 ($\sim 5\%$) and to the allylic hydroperoxide at C-8 (20). Whether the *bis*-allylic hydroperoxide at C-10 was subject to rearrangement was not reported. 11-HPODE is a poor substrate of sLO-1 (15), but huge amounts of sLO-1 (36,600 U/ml, ~ 0.25 mg/ml) catalyze the slow rearrangement of 11-HPODE (21).

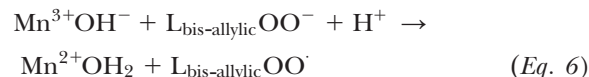
It is of interest to compare the rearrangement of *bis*-allylic hydroperoxides to *cis-trans* conjugated hydroperoxides during autoxidation and Mn-LOX catalysis, as the reaction mechanisms may differ. A key intermediate is the unstable *bis*-allylic peroxy radical, which transforms to an allylic peroxy radical via β -fragmentation and oxygenation at an allylic position during autoxidation (11, 12):



The LOO–H bond dissociation enthalpy is ~ 88 kcal/mol, and it is likely that LOO \cdot is formed during autoxidation by hydrogen abstraction by radical species (12). Mn-LOX catalyzes the rearrangement of *bis*-allylic hydroperoxides, likely by the formation of the *bis*-allylic peroxy radical, β -fragmentation, and oxygen insertion at the n-6 (or n-8) position under steric control by the enzyme.

How can *bis*-allylic peroxy radicals be generated from *bis*-allylic hydroperoxides by Mn-LOX? The mechanism is

likely related to the high redox potential of Mn^{3+} . It has been suggested that peroxy radicals might be generated from peroxide anions by the reduction of metal ions (22), suggesting the following hypothetical rearrangement mechanism for Mn-LOX:



The *bis*-allylic peroxy radical is then subjected to β -fragmentation and oxygen insertion under steric control by the enzyme, with formation of an allylic peroxy radical as discussed above. Recently, hypochloric acid (1 mM) was reported to convert allylic hydroperoxides of 18:2n-6 to peroxy radicals, but the mechanism is unknown (23). In contrast, homolytic cleavage of hydroperoxides has been studied extensively. Aqueous Fe^{2+} , other divalent metal ions, hematin, and the reduced forms of Fe-lipoxygenases and Mn-LOX can catalyze the homolytic cleavage of alkyl hydroperoxides (24, 25). Homolytic cleavage by Mn-LOX is influenced by the position of the hydroperoxide at the active site, as judged from the effects of substrate chain length and double bond configuration (25). It seemed

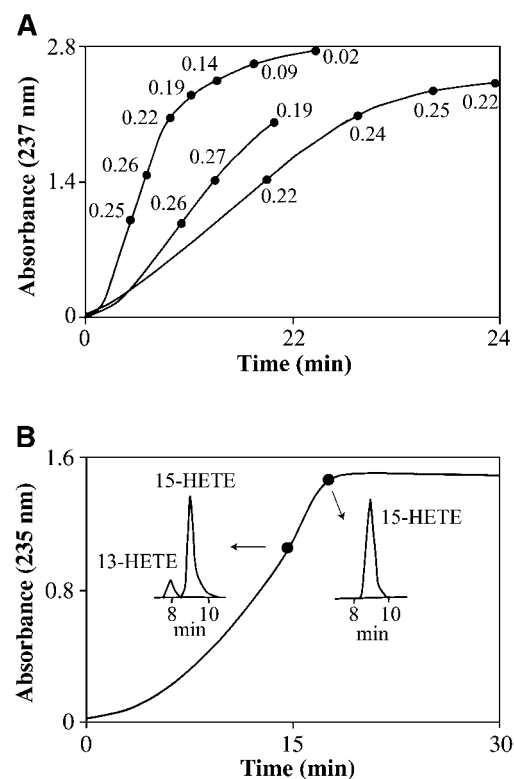


Fig. 1. Oxidation of 18:3n-3 and 20:4n-6 by manganese lipoxygenase (Mn-LOX). A: Progression curve with ultraviolet (UV) and LC-MS/MS analysis of products formed during the oxygenation of 18:3n-3 by Mn-LOX. Mn-LOX (19, 7, and 4 nM) was incubated with 18:3n-3, aliquots were analyzed for 11-hydroperoxyoctadecadienoic acid (11-HPODE) and 13-HPODE, and the ratio 11-HPODE/(11-HPODE + 13-HPODE) is indicated at these time points. B: Oxidation of 20:4n-6 by Mn-LOX (72 nM). The *bis*-allylic intermediate 13-hydroperoxyeicosatetraenoic acid (13-HPETE) was rapidly transformed to 15-HPETE, as indicated by MS/MS analysis at two time points at the upper end of the progression curve.

possible that these factors also might influence the rearrangement of *bis*-allylic hydroperoxides to allylic.

The aim of the present study was to study the factors controlling the rearrangement of *bis*-allylic hydroperoxides by Mn-LOX. The first goal was to confirm that the fatty acids bind "tail-first" in the active site of Mn-LOX during rearrangement in the same way as during oxygenation (26). The second goal was to determine the in-

fluence of the Gly316Ala mutant on the rearrangement reaction. This mutant changed the position of oxygenation and the interaction of the hydroperoxides with the catalytic metal (25). D₂O could be expected to increase the P_{K_a} for peroxide anions by 0.4, and this solvent deuterium isotope effect might conceivably reduce both the concentration of the anion and the rate of rearrangement. Finally, we investigated whether mutants of pre-

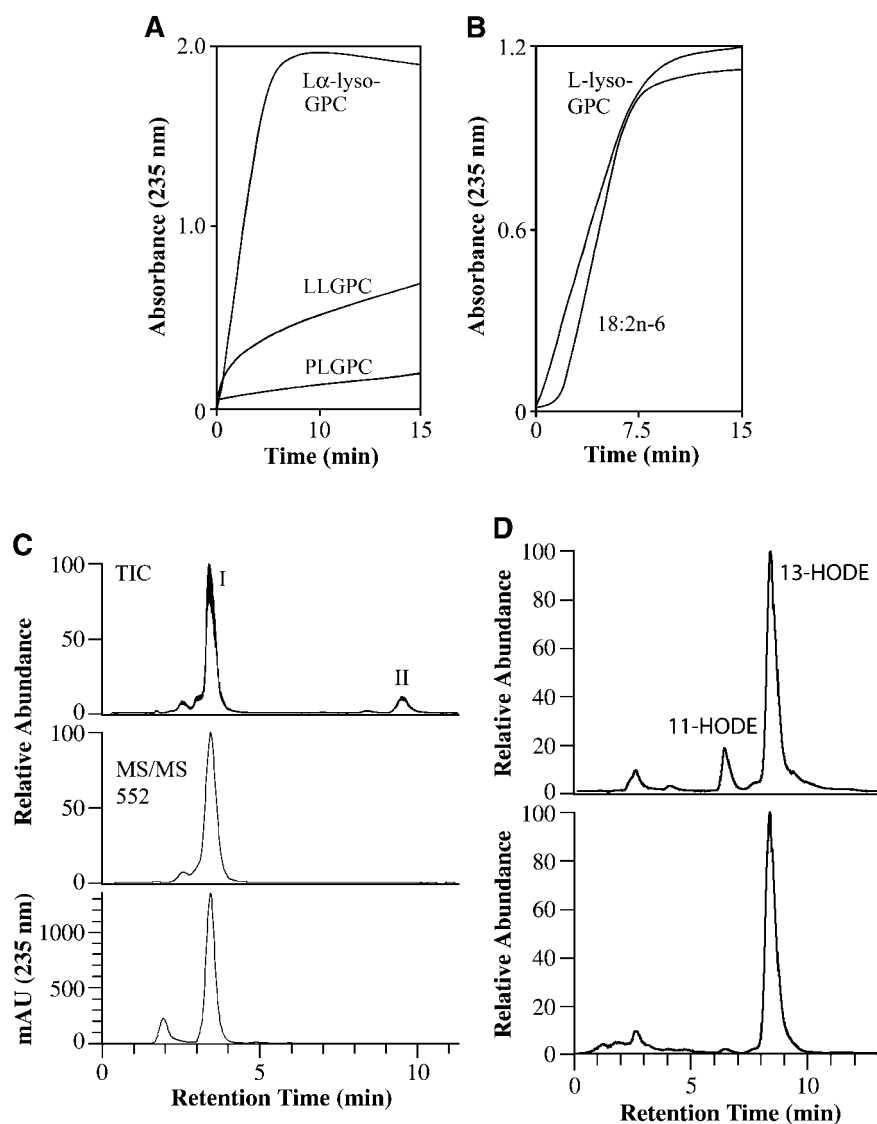


Fig. 2. Progression curves for the oxygenation of phosphatidylcholines by Mn-LOX to products with UV absorbance at 235 nm and LC-MS/MS analysis of products formed from 1-linoleoyl-lysoglycerophosphatidylcholine (1-linoleoyl-lysoGPC). A: Transformation of palmitate-linoleoyl-GPC (PLGPC), dilinoleoyl-GPC (LLGPC), and soybean L α -lysoGPC (L α -lysoGPC; containing ~42% 1-linoleoyl-lysoGPC and 10–15% 1-linolenoyl-lysoGPC) to products with UV absorbance at 235 nm by Mn-LOX. B: Comparison of the oxygenation of 18:2n-6 and 1-linoleoyl-lysoGPC (L-lysoGPC) by Mn-LOX (18 nM) and 50 μ M substrates. The direct oxidation to 13-HPODE was estimated from UV analysis (235 nm), and the relative amounts of 13-HPODE and 11-HPODE in oxidized 1-linoleoyl-lysoGPC were determined by treatment with cholesteryl esterase followed by LC-MS/MS analysis. C: Reverse phase (RP)-HPLC-MS/MS analysis of dioxygenated products formed from 1-linoleoyl-lysoGPC by Mn-LOX. UV and MS/MS analysis of peak I was consistent with 1-(13-hydroperoxyoctadeca-9Z,11E-dienoate)-lysoGPC, and peak II was consistent with 1-linoleoyl-lysoGPC. TIC, total ion current. D: Analysis of hydroxy fatty acids produced during the oxidation of 1-linoleoyl-lysoGPC with Mn-LOX at the linear phase (top) and at the plateau (bottom; cf. B) and obtained by cleavage with cholesteryl esterase. The chromatograms show total ion current.

sumed amino acids of the first and second coordinating spheres in a hydrogen bond network might affect the rearrangement. Asn694 and Glu697 of sLO-1 belong to this group of amino acids (4), and the homologous residues of Mn-LOX are Asn466 and Ser469 (18, 19).

EXPERIMENTAL PROCEDURES

Materials

1-Palmitoyl-2-linoleoyl-glycerophosphatidylcholine (GPC; 99%), L α -lysoGPC (from soybean; 99%), dilinoleoyl-GPC (99%), 20:2n-6 (99%), 20:3n-3 (99%), and 20:4n-6 (99%) were obtained from Larodan (Malmö, Sweden). 18:2n-6 (99%), 18:3n-6 (99%), and HPLC solvents (Lichrosolve) were from Merck. Fatty acids were dissolved in ethanol and stored in stock solutions (50–100 mM) at -20°C ; fresh solutions (50–150 μM) of the fatty acids were usually prepared in 0.1 M NaBO₃ buffer (pH 9.0). Phospholipase A₂ (bee venom), cholesteryl esterase (porcine pancreas), and ²H₂O (99.98%) were from Sigma-Aldrich. Site-directed mutagenesis of Mn-LOX was performed as described, and the expression constructs were sequenced (19). Amino acids of Mn-LOX were numbered after cleavage of the N-terminal secretion signal of 16 amino acids from the Mn-LOX precursor of 618 amino acids (GenBank AAK81862) and the secreted enzyme of 602 amino acids was expressed (19). Recombinant Mn-LOX, Mn-LOX G316A, Mn-LOX N466L, and Mn-LOX S469A were expressed in *Pichia pastoris* (strain X-33) as secreted proteins using the expression vector pPICZA α (19). The recombinant enzymes were purified from the growth medium by hydrophobic interaction chromatography as described (14, 19), concentrated by diafiltration, and stored at $+4^{\circ}\text{C}$.

Mn-LOX assay

Light absorbance was measured with a dual-beam spectrophotometer (Shimadzu UV-2101PC) with a 1 cm path length. The *cis-trans* conjugated hydro(pero)xy fatty acids were assumed to have an extinction coefficient of 25,000 $\text{cm}^{-1}\text{M}^{-1}$ (27). Lipoygenase activity was monitored by ultraviolet (UV) spectroscopy (235–237 nm) in 0.1 M NaBO₃ buffer (pH 9.0) with 50–120 μM substrate. Reaction was started by the addition of Mn-LOX. Oxygenated fatty acids were usually analyzed after extractive isolation (SepPak/C₁₈; Waters) without acidification (19) and oxygenated 1-linoleoyl-lysoGPC after Folch extraction. The fatty acid hydroperoxides and keto fatty acids were reduced to alcohols by treatment with NaBH₄ or NaB²H₄ before LC-MS/MS analysis, unless stated otherwise. Mn-LOX was prepared in D₂O buffer by repeated diafiltration (30 k; Amicon Ultra; Millipore) and added (in <1% volume) to 65 μM 11-hydroperoxyoctadecatrienoic acid (11-HPOTrE) in 0.1 M NaHPO₄ (pD 7.5 and pH 7.5). pH was measured with glass electrodes from Radiometer Copenhagen. Because of the solvent isotope effect of deuterium oxide on pH glass electrodes, pD was calculated as measured pH plus 0.4 (28).

HPLC-MS/MS

Reverse phase (RP)-HPLC with MS/MS analysis was performed with a Surveyor MS pump (Thermo) and with an octadecyl silica column (5 μm ; 2.1 \times 150 mm; Phenomenex or Hypersil Gold), which was usually eluted with methanol-water-acetic acid (750:250:0.06; Suprapur; Merck) at 0.3 ml/min. The effluent passed a photodiode array detector (Surveyor PDA; 5 cm path length) and was subjected to electrospray ionization in an ion trap mass spectrometer (LTQ; Thermo). The heated transfer capillary was set at 315 $^{\circ}\text{C}$, the ion isolation width at 1.5 amu, and the collision

energy at 25–35 (arbitrary scale). Prostaglandin F_{1 α} (100 ng/min) was infused for tuning. 1-Linoleoyl-lysoGPC and its metabolites were separated on the Hypersil Gold column, which was eluted with acetonitrile-5 mM ammonium acetate (35:65) at 0.3 ml/min, with UV detection and MS/MS monitoring of positive ions.

Normal phase (NP)-HPLC with MS/MS analysis was performed on silica with an analytical column (Kromasil-100SI; 250 \times 2 mm, 5 μm , 100 Å), which was eluted at 0.3 ml/min with 5% isopropanol in hexane with 0.05 ml/l acetic acid (Constrametric 3200 pump; LDC). The effluent was combined with isopropanol-water (3:2; 0.2 ml/min) from a second pump (Surveyor MS pump) as described (26). The combined effluents were introduced by electrospray into the ion trap mass spectrometer (LTQ). Chiral phase (CP)-HPLC was performed with Chiralcel OD (25 \times 0.46 cm; Daicel through Skandinaviska GeneTech, Kungälv, Sweden) and eluted with 5% isopropanol in hexane with 0.1% acetic acid (0.5 ml/min). The effluent was analyzed by photodiode array detection, mixed with isopropanol-water (3:2; 0.3 ml/min), and subjected to MS/MS analysis of carboxylate anions.

Miscellaneous

11-HPOTrE was isolated from incubations of 20–200 ml of 0.1 M NaBO₃ buffer (pH 9.0) with 100 μM 18:3n-3 and ~ 4 nM

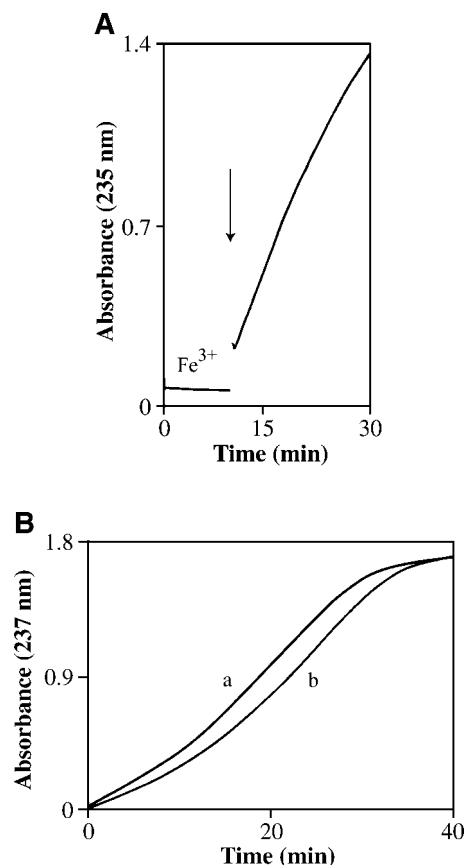


Fig. 3. UV analysis of 11-hydroperoxyoctadecatrienoic acid (11-HPOTrE) treated with aqueous Fe³⁺ and with Mn-LOX in H₂O and D₂O buffers. A: Ten micromolar Fe³⁺ did not increase the UV absorbance at 237 nm, and experiments with 30 and 100 μM yielded similar results. Mn-LOX was added as indicated by the arrow. B: Kinetic traces from incubation of 65 μM 11-HPOTrE with Mn-LOX (7 nM) in 0.1 M sodium phosphate buffer in H₂O (pH 7.5; trace a; median trace of five replicas) and D₂O (pD 7.5; trace b; median trace of five replicas).

Mn-LOX when the linear increase in UV absorbance started to deviate. The products were extracted with cold ethyl acetate, evaporated to dryness, and purified by RP-HPLC [methanol-water-acetic acid, 750:250:0.1; 4.2×100 mm, $5 \mu\text{m}$ Hypersil Gold (Thermo) or $10 \mu\text{m}$, 8×300 mm, $\mu\text{Bondapak C18}$ (Waters)], with UV detection at 210 and 237 nm. Fractions containing 11-HPOTrE were extracted with CH_2Cl_2 and evaporated to dryness, and the amount of 11-HPOTrE was estimated by UV analysis after conversion of an aliquot to 13-HPOTrE with Mn-LOX. 1-Linoleoyl-lysoGPC was obtained by treatment of dilinoleoyl-GPC with phospholipase A_2 , purified by preparative TLC ($\text{CHCl}_3/\text{methanol}/\text{NH}_3/\text{H}_2\text{O}$, 6:3.6:0.4:0.4; $R_f \sim 0.23$), and characterized by RP-HPLC-MS/MS analysis. Hydrolysis of oxygenated 1-linoleoyl-lysoGPC was performed with cholesteryl esterase as described (29).

RESULTS AND DISCUSSION

18:3n-3 was rapidly oxidized by Mn-LOX, as shown by Fig. 1A, and the kinetic parameters ($K_m = 2.4 \mu\text{M}$, $V_{max} = 17.6 \mu\text{mol}/\text{min}/\text{mg}$, and $k_{cat} = 2,400 \text{ min}^{-1}$) have been reported previously (14). During the rapid linear phase of biosynthesis of UV light-absorbing products at 237 nm (13-HPOTrE, traces of 9-HPOTrE), the apparent amounts of the two main products were estimated by LC-MS/MS analysis. 11-HPOTrE averaged 25% (range, 22–27%), and 13-HPOTrE averaged $\sim 75\%$. The first linear increase in UV absorbance was followed by a second linear phase (at a rate of 13–15% of the first), during which 11-HPOTrE was converted to 13-HPOTrE (15). The rearrangement of 11-HPOTrE occurred slowly when low amounts of enzyme

were used (4 nM Mn-LOX; Fig. 1A), which provided a practical way to generate 11-HPOTrE.

20:4n-6 is a poor substrate of Mn-LOX and required large amounts of enzyme for rapid transformation (25, 26). Oxidation of 20:4n-6 by Mn-LOX and analysis of the products are illustrated in Fig. 1B. Analysis of the products during the rapid and almost linear increase in UV absorbance at 235 nm, which is attributable mainly to the formation of 15*R*-hydroperoxy-5*Z*,8*Z*,11*Z*,13*E*-eicosatetraenoic acid (15-HPETE) (26), showed that 13-hydroperoxy-5*Z*,8*Z*,11*Z*,14*Z*-eicosatetraenoic acid (13-HPETE) accounted for $\sim 10\text{--}14\%$ of the products during the upper part of the linear phase. This number was below 1% already at the peak of UV absorbance and was $<0.1\%$ at later time points (data not shown). In comparison with 20:3n-3, the *bis*-allylic hydroperoxide of 20:4n-6 was rearranged rapidly.

Oxygenation of dilinoleoyl-GPC suggested that fatty acids bind the active site of Mn-LOX tail-first (26), but it has not been confirmed whether *bis*-allylic hydroperoxides bind in the same way for rearrangement. Mn-LOX oxidized soybean L_α -lysoGPCs much more efficiently than 1-palmitoyl-2-linoleoyl-GPC and dilinoleoyl-GPC (Fig. 2A). Homolytic cleavage of hydroperoxides of L_α -lysoGPCs to keto fatty acids occurred at the end of lipoxygenation, as judged from a decrease in UV absorbance at 235 nm and an increase in UV absorbance with a broad maximum at 280 nm (isobestic point of 259 nm). Analysis of oxygenated fatty acids after NaBH_4 reduction and hydrolysis (0.5 M KOH in methanol) showed that 13-hydroxyoctadecadienoic acid (13-HODE) and 13-hydroxyoctadecatrienoic acid were

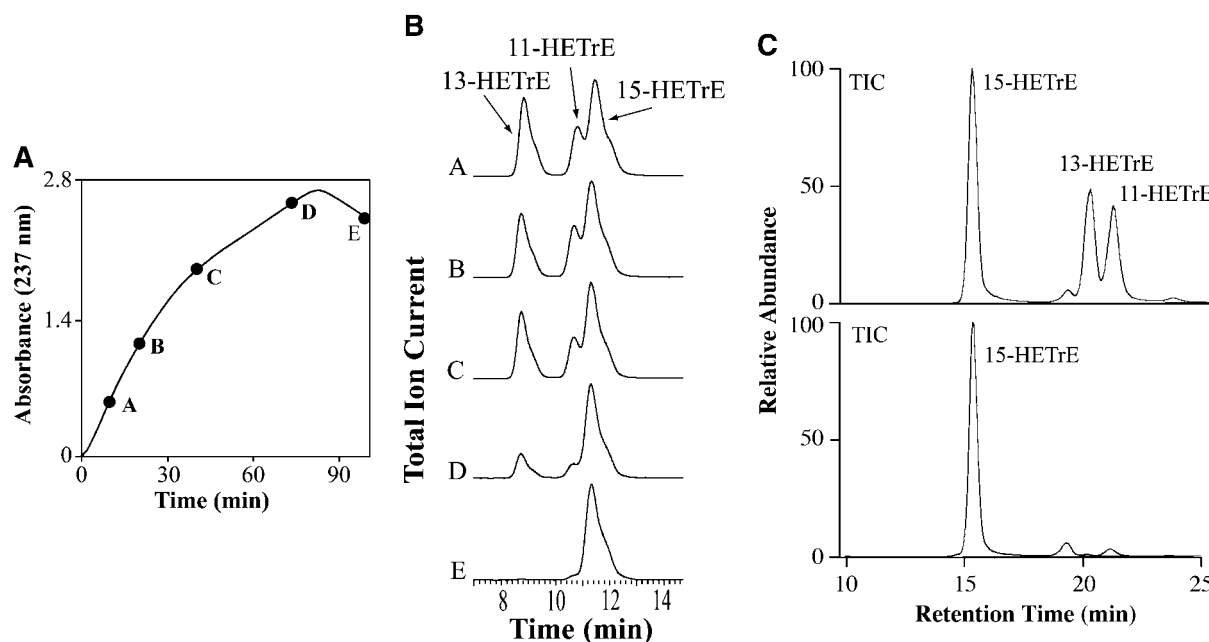


Fig. 4. Oxygenation of 20:3n-3 by Mn-LOX. A: A kinetic trace with analysis of products at time points A–E formed from 20:3n-3 by 72 nM Mn-LOX. The solid line shows the UV absorbance at 237 nm attributable to the biosynthesis of allylic hydroperoxides [15-hydroperoxyeicosatrienoic acid (HPETrE) and 11-HPETrE], and the time points (A–E) mark where aliquots were taken for analysis of the oxygenated metabolites by LC-MS/MS. B: LC-MS/MS analysis of 11-, 13-, and 15-HETrE at time points A–E after reduction with NaBH_4 . C: Normal phase (NP)-HPLC-MS/MS analysis of products formed during the linear increase of UV absorbance (top) and at the end of lipoxygenation (bottom). TIC, total ion current.

formed, but 11-hydroxy metabolites could not be detected under these harsh conditions.

1-Linoleoyl-lysoGPC was oxidized by Mn-LOX almost as efficiently as 18:2n-6 (Fig. 2B). LC-MS/MS analysis and UV analysis showed that 1-linoleoyl-lysoGPC was oxidized by Mn-LOX to a hydroperoxy metabolite with UV absorbance maximum at 235 nm (Fig. 2C). A slightly more polar metabolite lacking significant UV absorbance at 235 nm was also formed. The MS/MS spectrum of the main metabolites (m/z 552 \rightarrow full scan) showed signals attributable to the sequential loss of one, two, and three molecules of water [m/z 534 (base peak), 516, and 498, respectively] and possibly the loss of H_2O_2 (m/z 518) from $[M+H]^+$. Signals

were also noted at m/z 452, 434, and 184. The MS/MS spectrum and the UV analysis were consistent with the formation of a 13-hydroperoxy metabolite of 1-linoleoyl-lysoGPC. *bis*-Allylic oxidation of 1-linoleoyl-lysoGPC by Mn-LOX and hydroperoxide rearrangement were finally demonstrated by treatment with cholesteryl esterase, which yielded a mixture of 11-HODE and 13-HODE during the linear oxidation phase but only 13-HODE at the end of lipoxygenation (Fig. 2D).

We next examined the transformation of 11-HPOTrE to 13-HPOTrE by Fe^{3+} . 11-HPOTrE was incubated with $10 \mu M$ Fe^{3+} , and the UV absorbance at 237 nm was followed for 10 min, but it remained unchanged (Fig. 3A). The pres-

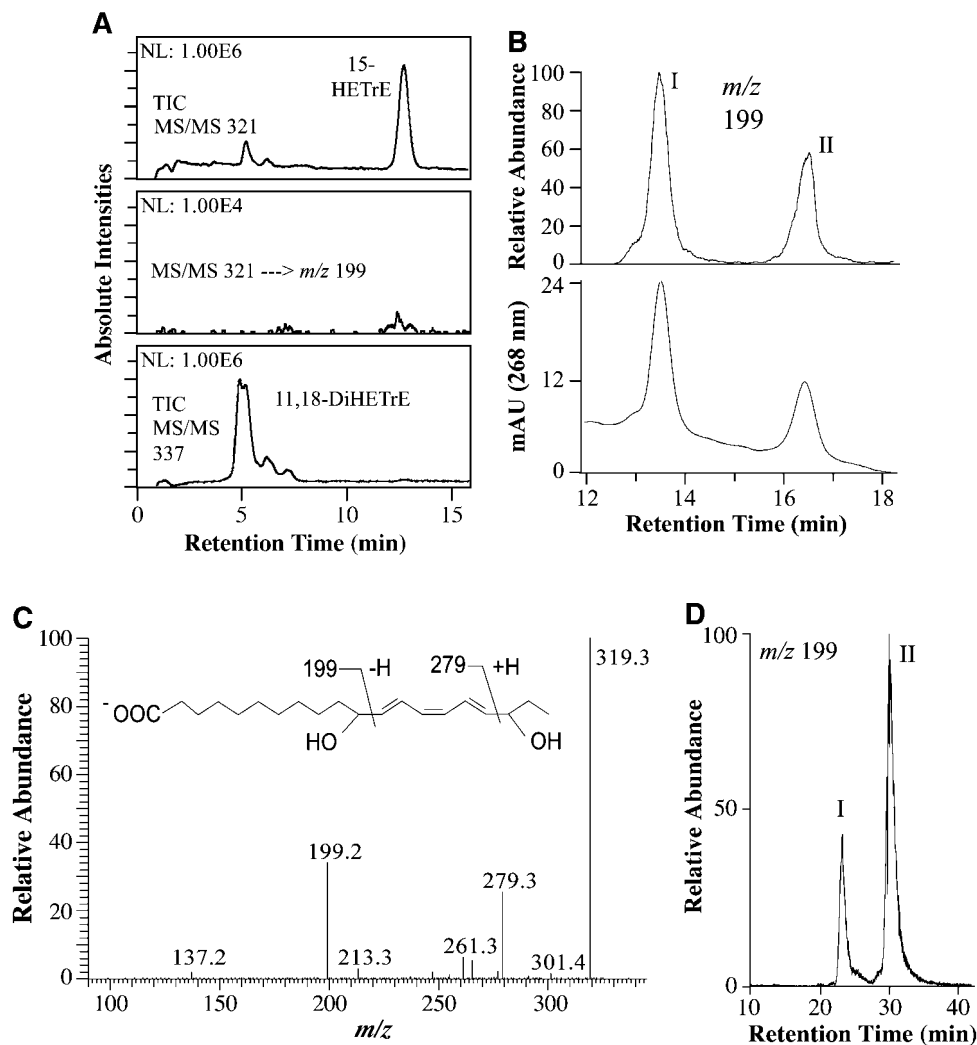


Fig. 5. RP-HPLC- and NP-HPLC-MS/MS analysis of 15-HETrE, 11-HETrE, and 11,18-dihydroxyeicosatrienoic acid (DiHETrE) at the end of lipoxygenation. A: RP-HPLC-MS/MS analysis of products. Top, total ion current (TIC) of MS/MS analysis (m/z 321 \rightarrow full scan); the main peak with a retention time of 13 min contained 15-HETrE. Middle, reconstructed ion chromatogram of the characteristic fragment of 11-HETrE during MS/MS analysis (m/z 321 \rightarrow m/z 199) magnified 100 times. Bottom, total ion current of MS/MS analysis (m/z 337 \rightarrow full scan); the main peak contained 11,18-DiHETrE. NL, normalized to intensity as indicated. B: Separation of diastereoisomers of 11,18-DiHETrE by NP-HPLC and analysis by MS/MS (m/z 337 \rightarrow full scan) and by UV light (268 nm). MS/MS and UV analysis suggested that peaks I and II contained diastereoisomers of 11,18-DiHETrE. C: MS/MS spectrum (m/z 337 \rightarrow full scan) of 11,18-DiHETrE. The inset shows the carboxylate anion and formation of the major fragment ions as indicated. D: Reconstructed ion chromatogram for steric analysis of 11-HETrE by chiral phase-HPLC-MS/MS with monitoring of the characteristic signal at m/z 199. MS/MS analysis showed that peaks marked I and II contained 11-HETrE.

ence of 11-HPOTrE was confirmed by the addition of Mn-LOX, which rapidly transformed 11-HPOTrE to 13-HPOTrE, as indicated in Fig. 3A. Higher concentrations of Fe^{3+} (30 and 100 μM) were also without noticeable effect, even after long incubation times. It would have been more appropriate to investigate the effect of Mn^{3+} on 11-HPOTrE. Mn^{3+} has a higher redox potential than Fe^{3+} ($\text{Mn}^{2+} \leftrightarrow \text{Mn}^{3+} + \text{e}^-$, ~ 1.5 V; $\text{Fe}^{2+} \leftrightarrow \text{Fe}^{3+} + \text{e}^-$, 0.77 V). Unfortunately, Mn^{3+} is unstable in aqueous solutions and forms MnO_2 and Mn^{2+} .

The solvent deuterium isotope effect on sLO-1 kinetics has been thoroughly investigated (4, 30). Substituting H_2O with D_2O has virtually no effect on the k_{cat} of sLO-1 at room temperature (30). The solvent deuterium isotope effect on the rearrangement of *bis*-allylic hydroperoxides has not been studied. Figure 3B illustrates the rearrangement of 11-HPOTrE by Mn-LOX in 0.1 M NaHPO_4 (pH 7.5 and pD 7.5). After an initial kinetic lag phase, during which Mn-LOX likely was fully transformed to its active form by the produced 13-HPOTrE, the linear rate of oxygenation appeared to be virtually identical in the two solvents. The kinetic lag phase was not observed when a 1:1 mixture of 11- and 13-HPOTrE was used as substrate. The rationale for this experiment was that the pK_a of 11-HPOTrE should increase by 0.4 in D_2O , thus reducing the concentration of the peroxide anion available for reduction by Mn^{3+} -LOX. We cannot exclude that a distinct solvent isotope effect on k_{cat} might be present at a lower pL [-log (molar concentration of H^+ and D^+)], but 11-HPOTrE is chemically unstable at acidic pH (31).

We next examined the effect of substrate chain length on *bis*-allylic hydroxylation and rearrangement. 20:2n-6 was oxygenated to 15-hydroperoxy-9Z,11E-hydroxyeicosadienoic acid (15-HEDE) as the main product and to 11-hydroperoxy-10E,12Z-eicosadienoic acid (11-HEDE; a low percentage). 13-Hydroperoxy-9Z,12Z-eicosadienoic acid (13-HEDE) could not be detected by MS/MS analysis during the linear phase of oxidation.

20:3n-3 was oxidized by Mn-LOX to 13-, 11-, and 15-hydroperoxyeicosatrienoic acids (HPETrEs), as shown in Fig. 4A. The hydroxylated products were analyzed at five time points (Fig. 4A), and the results are shown in Fig. 4B. 15-Hydroperoxy-11Z, 13E, 17Z-eicosatrienoic acid (15-HETrE) accumulated as one end product. 13-Hydroperoxy-11Z, 14Z, 17Z-eicosatrienoic acid (13-HPETrE) was apparently rearranged to 15-HETrE, and 11-hydroperoxy-12E, 14Z, 17Z-eicosatrienoic acid (11-HPETrE) was also transformed to other products. NP-HPLC-MS/MS and UV analysis showed that 15-HETrE was the main product (Fig. 4C). The isomer of 15-HETrE with the 9E,11E configuration could not be detected. This ruled out the possibility that 11-HPETrE was subject to hydroperoxide rearrangement.

Mn-LOX oxidizes 16:3n-3 at the n-3 position with the *R* configuration (26), and this was also apparently the case with 11-HPOTrE. 11-HPOTrE was oxidized by Mn-LOX to two diastereoisomers of 11,18-dihydroxy-12E, 14Z, 16E eicosatrienoic acid (DiHETrE), as indicated by RP-HPLC-MS/MS and UV analysis (Fig. 5A). The UV spectrum showed an absorbance maximum at 268 nm with shoulders at 260

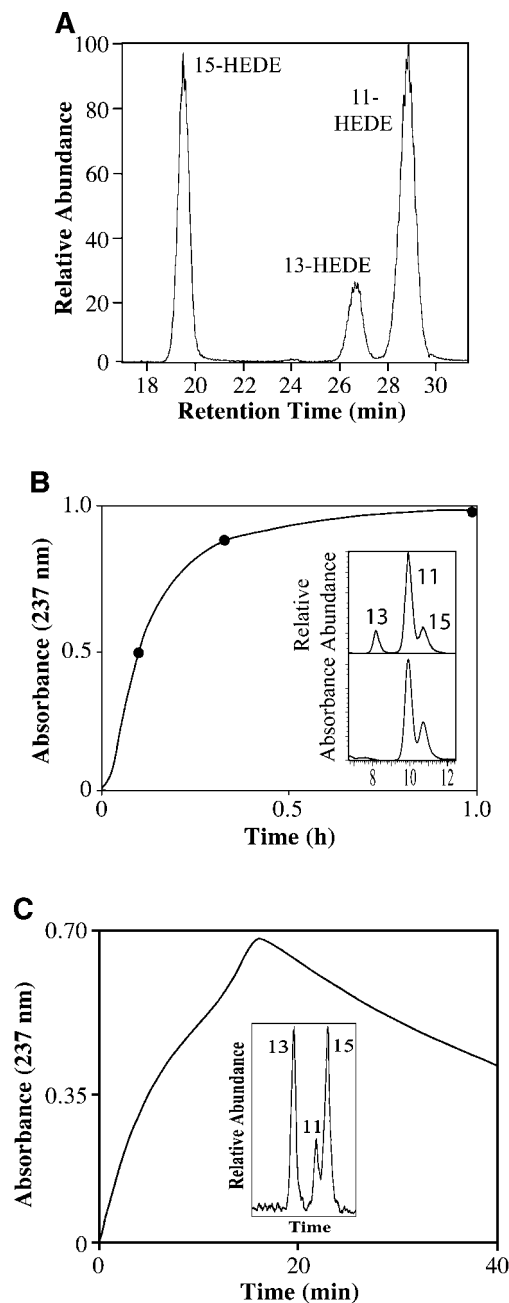


Fig. 6. Oxygenation of 20:2n-6 and 20:3n-3 by Mn-LOX G316A and 20:3n-3 by S469A. A: NP-HPLC-MS/MS analysis of products formed from 20:2n-6 by Gly316Ala. The oxygenation at C-11 and C-13 is insignificant by the native enzyme, which illustrates that oxygenation was shifted toward the carboxyl group. B: Oxidation of 20:3n-3 by Gly316Ala. The oxygenation is shifted toward C-13 and C-11 [inset with MS/MS analysis (top) and UV analysis at 237 nm (bottom)]. The rearrangement of 13-HPETE to 15-HPETE appeared to be blocked, as product analysis at the three indicated time points yielded virtually identical amounts of 11-, 13-, and 15-HETrE and there was no indication of a significant homolytic cleavage of 15-HPETE (no decline in UV absorbance at 237 nm). C: Oxygenation of 20:3n-3 by Ser469Ala. The inset shows the relative amounts of hydroxy metabolites during the initial phase of oxygenation. The kinetic trace appeared to be identical to that of the native enzyme. 13, 11, and 15 denote 13-H(P)ETrE, 11-H(P)ETrE, and 15-H(P)ETrE in the insets of B and C.


and 279 nm, suggesting a triene configuration of double bonds. The two diastereoisomers were resolved by NP-HPLC in a 2:1 ratio, as shown in Fig. 5B. The UV and MS/MS spectra of both products were identical. MS/MS analysis (m/z 337 \rightarrow full scan) showed informative signals at m/z 199 [$^-$ OOC-(CH₂)₉-COH] and m/z 279 [$^-$ OOC-(CH₂)₉-CHOH-CH=CH-CH=CH-CH=CH-COH], as shown in Fig. 5C. CP-HPLC-MS/MS analysis suggested that 11-HPETrE was formed as a 1:2 mixture of two stereoisomers (Fig. 5D), and both appeared to be quantitatively transformed to 11,18-DiHETrE. The elution order of the stereoisomers of 11,18-DiHETrE on NP-HPLC and 11-HETrE on CP-HPLC was not determined, but 11*R*-hydroxyeicosatetraenoic acid elutes before 11*S*-hydroxyeicosatetraenoic acid on Chiralcel OD (32).

The main difference between Mn-LOX and its Gly316Ala mutant was an augmented hydroperoxide isomerase activity, with formation of epoxyalcohols and keto fatty acids of 13*R*-hydroperoxides of 18:3*n*-3 and 18:2*n*-6, and a modest shift in the position of oxidation toward the carboxyl group (25). The Gly316Ala mutant had pronounced effects on the positions of oxidation of 20:2*n*-6 and 20:3*n*-3. This mutant oxidized 20:2*n*-6 at all three positions, C-11, C-13, and C-15, as shown by NP-HPLC-MS/MS analysis of products during the linear increase in UV absorbance at 235 nm (Fig. 6A). 13-HEDE was rearranged to 15-HEDE at the end of lipoxygenation (data not shown). The Gly316Ala mutant oxidized 20:3*n*-3 mainly at C-11 and to some extent at C-13 and C-15 (inset in Fig. 6B). However, the rearrangement of 13-HPETrE to 15-HPETrE, the oxygenation of 11-HPETrE to 11,18-DiHETrE, and the homolytic cleavage of 15-HPETrE to 15-keto-11*Z*,14*E*,17*Z*-eicosatrienoic acid appeared to be much slower than with the native enzyme, as judged from the progression curve and MS/MS analysis (Fig. 6B and inset). Although Gly316Ala oxidized both 20:2*n*-6 and 20:3*n*-3 at C-11, C-13, and C-15, the rearrangement of the *bis*-allylic hydroperoxides at C-13 differed.

Lipoxygenases contain three conserved residues in the sequence HxxxNxxQ. The histidine residue is an iron and manganese ligand, which is conserved along with the glutamine residue in Fe-lipoxygenases [the LOX-DB at www.dkfz-heidelberg.de/spec/lox-db/, as described (33)]. The Asn694 residue in this sequence of sLO-1 belongs to the first coordinating sphere, and a hydrogen bond network has been identified between Asn694 and two residues of the second coordinating sphere, Gln697 and Gln495 (4). Asn694 and Gln495 are conserved in Mn-LOX as Asn466 and Gln281, whereas Ser469 is present in the homologous position of Gln697. We assessed whether Asn466 and Ser469 of the presumed first and second coordinating spheres affected the rearrangement of *bis*-allylic hydroperoxides.

Mn-LOX S469A metabolized 18:2*n*-6, 18:3*n*-3, 20:2*n*-6, and 20:3*n*-3 to the same profile of metabolites as Mn-LOX. The oxidation of 20:3*n*-3 is shown in Fig. 6C. Mn-LOX Asn466Leu possessed only low lipoxygenase activity, as reported previously (19). 18:2*n*-6 and 18:3*n*-3 were oxidized to the same products as by the native enzyme,

and the 11-hydroperoxides of 18:2*n*-6 and 18:3*n*-3 were transformed to 13-hydroperoxides at the end of lipoxygenation. 20:2*n*-6 was transformed to 15-HEDE and ~5% 13-HEDE with rearrangement to 15-HEDE at the end of lipoxygenation. We conclude that Gly316 is important for the interaction of 13-HPETrE with the catalytic metal, whereas neither Asn466 nor Ser469 has major effects on the rearrangement of several *bis*-allylic hydroperoxides.

Rearrangement of *bis*-allylic hydroperoxides and homolytic cleavage of hydroperoxides are likely catalyzed by Mn³⁺-LOX and Mn²⁺-LOX, respectively, and both reactions can be influenced by alignment of the *bis*-allylic and allylic hydroperoxides. The position of the *bis*-allylic hydroperoxide and the allylic hydroperoxide in the vicinity of the catalytic metal appears to be essential. The Gly316Ala mutant, substrate chain length, and double bond configuration affected both reactions, whereas mutation of Ser469 had little effect on the homolytic cleavage of 15-HPETrE or on the rearrangement of 13-HPETrE. It seems likely that Mn-LOX catalyzes direct electron transfer from the *bis*-allylic hydroperoxide anion to the catalytic base Mn³⁺OH⁻ with subsequent generation of Mn²⁺OH₂, the resting form of Mn-LOX. The kinetic trace for the rearrangement of 11-HPOTrE to 13-HPOTrE shows a distinct kinetic lag phase in support of this mechanism. 

This work was supported by Vetenskapsrådet Medicin (Grant 03X-06523) and Formas (Grant 222-2005-1733). Expert help with the Mn-LOX mutants by Dr. M. Cristea (Swedish Agricultural University, Uppsala) and generous advice by Dr. M. Hamberg (Karolinska Institutet, Stockholm) are gratefully acknowledged.

REFERENCES

1. Brash, A. R. 1999. Lipoxygenases: occurrence, functions, catalysis, and acquisition of substrate. *J. Biol. Chem.* **274**: 23679–23682.
2. Kuhn, H., J. Saam, S. Eibach, H. G. Holzthütter, I. Ivanov, and M. Walther. 2005. Structural biology of mammalian lipoxygenases: enzymatic consequences of targeted alterations of the protein structure. *Biochem. Biophys. Res. Commun.* **338**: 93–101.
3. Liavonchanka, A., and I. Feussner. 2006. Lipoxygenases: occurrence, functions and catalysis. *J. Plant Physiol.* **163**: 348–357.
4. Tomchick, D. R., P. Phan, M. Cymborowski, W. Minor, and T. R. Holman. 2001. Structural and functional characterization of second-coordination sphere mutants of soybean lipoxygenase-1. *Biochemistry*. **40**: 7509–7517.
5. Lehnert, N., and E. I. Solomon. 2003. Density-functional investigation on the mechanism of H-atom abstraction by lipoxygenase. *J. Biol. Inorg. Chem.* **8**: 294–305.
6. Hammes-Schiffer, S. 2006. Hydrogen tunneling and protein motion in enzyme reactions. *Acc. Chem. Res.* **39**: 93–100.
7. Hatcher, E., A. V. Soudackov, and S. Hammes-Schiffer. 2007. Proton-coupled electron transfer in soybean lipoxygenase: dynamical behavior and temperature dependence of kinetic isotope effects. *J. Am. Chem. Soc.* **129**: 187–196.
8. Rickert, K. W., and J. P. Klinman. 1999. Nature of hydrogen transfer in soybean lipoxygenase 1: separation of primary and secondary isotope effects. *Biochemistry*. **38**: 12218–12228.
9. Kitaguchi, H., K. Ohkubo, S. Ogo, and S. Fukuzumi. 2006. Additivity rule holds in the hydrogen transfer reactivity of unsaturated fatty acids with a peroxyl radical: mechanistic insight into lipoxygenase. *Chem. Commun. (Camb.)*. 979–981.
10. Chan, D. W-S., G. Levett, and J. A. Mathew. 1979. The mechanism of the rearrangement of linoleate hydroperoxides. *Chem. Phys. Lipids*. **24**: 245–256.

11. Brash, A. R. 2000. Autoxidation of methyl linoleate: identification of the bis-allylic 11-hydroperoxide. *Lipids*. **35**: 947–952.
12. Pratt, D. A., J. H. Mills, and N. A. Porter. 2003. Theoretical calculations of carbon-oxygen bond dissociation enthalpies of peroxy radicals formed in the autoxidation of lipids. *J. Am. Chem. Soc.* **125**: 5801–5810.
13. Tallman, K. A., D. A. Pratt, and N. A. Porter. 2001. Kinetic products of linoleate peroxidation: rapid beta-fragmentation of nonconjugated peroxy radicals. *J. Am. Chem. Soc.* **123**: 11827–11828.
14. Su, C., and E. H. Oliw. 1998. Manganese lipoxygenase. Purification and characterization. *J. Biol. Chem.* **273**: 13072–13079.
15. Hamberg, M., C. Su, and E. Oliw. 1998. Manganese lipoxygenase. Discovery of a bis-allylic hydroperoxide as product and intermediate in a lipoxygenase reaction. *J. Biol. Chem.* **273**: 13080–13088.
16. Su, C., M. Sahlén, and E. H. Oliw. 2000. Kinetics of manganese lipoxygenase with a catalytic mononuclear redox center. *J. Biol. Chem.* **275**: 18830–18835.
17. Gaffney, B. J., C. Su, and E. H. Oliw. 2001. Assignment of EPR transitions in a manganese-containing lipoxygenase and prediction of local structure. *Appl. Magn. Reson.* **21**: 413–424.
18. Hörnsten, L., C. Su, A. E. Osbourn, U. Hellman, and E. H. Oliw. 2002. Cloning of the manganese lipoxygenase gene reveals homology with the lipoxygenase gene family. *Eur. J. Biochem.* **269**: 2690–2697.
19. Cristea, M., Å. Engström, C. Su, L. Hörnsten, and E. H. Oliw. 2005. Expression of manganese lipoxygenase in *Pichia pastoris* and site-directed mutagenesis of putative metal ligands. *Arch. Biochem. Biophys.* **434**: 201–211.
20. Boutaud, O., and A. R. Brash. 1999. Purification and catalytic activities of the two domains of the allene oxide synthase-lipoxygenase fusion protein of the coral *Plexaura homomalla*. *J. Biol. Chem.* **274**: 33764–33770.
21. Oliw, E. H., M. Cristea, and M. Hamberg. 2004. Biosynthesis and isomerization of 11-hydroperoxylinoleates by manganese- and iron-dependent lipoxygenases. *Lipids*. **39**: 319–323.
22. Davies, M. J., and T. F. Slater. 1987. Studies on the metal-ion and lipoxygenase-catalysed breakdown of hydroperoxides using electron-spin-resonance spectroscopy. *Biochem. J.* **245**: 167–173.
23. Miyamoto, S., G. R. Martinez, D. Rettori, O. Augusto, M. H. Medeiros, and P. Di Mascio. 2006. Linoleic acid hydroperoxide reacts with hypochlorous acid, generating peroxy radical intermediates and singlet molecular oxygen. *Proc. Natl. Acad. Sci. USA.* **103**: 293–298.
24. Yu, Z., C. Schneider, W. E. Boeglin, L. J. Marnett, and A. R. Brash. 2003. The lipoxygenase gene ALOXE3 implicated in skin differentiation encodes a hydroperoxide isomerase. *Proc. Natl. Acad. Sci. USA.* **100**: 9162–9167.
25. Cristea, M., and E. H. Oliw. 2006. A G316A mutation of manganese lipoxygenase augments hydroperoxide isomerase activity: mechanism of biosynthesis of epoxyalcohols. *J. Biol. Chem.* **281**: 17612–17623.
26. Cristea, M., and E. H. Oliw. 2007. On the singular, dual, and multiple positional specificity of manganese lipoxygenase and its G316A mutant. *J. Lipid Res.* **48**: 890–903.
27. Graff, G., L. A. Anderson, and L. W. Jaques. 1990. Preparation and purification of soybean lipoxygenase-derived unsaturated hydroperoxy and hydroxy fatty acids and determination of molar absorptivities of hydroxy fatty acids. *Anal. Biochem.* **188**: 38–47.
28. Salomaa, P., L. L. Schaleger, and F. A. Long. 1964. Solvent deuterium isotope effects on acid-base equilibria. *J. Am. Chem. Soc.* **86**: 1–7.
29. Huang, L. S., M. R. Kim, and D-E. Sok. 2006. Linoleoyl lysophosphatidylcholine is an efficient substrate for soybean lipoxygenase-1. *Arch. Biochem. Biophys.* **455**: 119–126.
30. Glickman, M. H., and J. P. Klinman. 1995. Nature of rate-limiting steps in soybean lipoxygenase-1 reaction. *Biochemistry.* **34**: 14077–14092.
31. Hamberg, M., W. H. Gerwick, and P. A. Åsén. 1992. Linoleic acid metabolism in the red alga *Lithothamnion corallioides*: biosynthesis of 11(R)-hydroxy-9(Z),12(Z)-octadecadienoic acid. *Lipids*. **27**: 487–493.
32. Meruvu, S., M. Walther, I. Ivanov, S. Hammarström, G. Fürstenberger, P. Krieg, P. Reddanna, and H. Kuhn. 2005. Sequence determinants for reaction specificity of the murine 12(R)-lipoxygenase. Targeted substrate modification and site directed mutagenesis. *J. Biol. Chem.* **280**: 36633–36641.
33. Lütteke, T., P. Krieg, G. Fürstenberger, and C. W. von der Lieth. 2003. LOX-DB—database on lipoxygenases. *Bioinformatics.* **19**: 2482–2483.